Modelling studies of HOM and its contributions to growth of new particles: comparison of boreal forest in Finland and polluted environment in China

Ximeng Qi[1,2,4], Aijun Ding[1,2*], Pontus Roldin[3,], Zhengning Xu[1,2], Putian Zhou[4], Nina Sarnela[4], Wei Nie[1,2],
Xin Huang[1,2], Anton Rusanen[4], Mikael Ehn[4], Matti P. Rissanen[4], Tuukka Petäjä[4,1], Markku Kulmala[4] and
Michael Boy[4]

[1]Joint International Research Laboratory of Atmospheric and Earth System Sciences, School of
Atmospheric Sciences, Nanjing University, Nanjing, 210023, China
[2]Collaborative Innovation Center of Climate Change, Nanjing, 210023, China
[3]Division of Nuclear Physics, Lund University, P.O. Box 118, 22100 Lund, Sweden
[4]Institute for Atmospheric and Earth System Research / Physics, Faculty of Science, University of
Helsinki, P.O. Box 64, 00014 University of Helsinki, Helsinki, Finland

Correspondence to: Aijun Ding (dingaj@nju.edu.cn)

Abstract. Highly oxygenated multifunctional compounds (HOM) play a key role in the growth of new particles during new particle formation (NPF) events, but their quantitative roles in different environments of the globe haven't been well studied yet. In this study, the HOM concentrations and NPF events at a remote boreal forest site in Finland (SMEAR II) and a sub-urban site in the polluted eastern China (SORPES) were simulated with the MALTE-BOX model, and their roles in NPF at the two distinctly different environments are discussed. We found that sulfuric acid and HOM organonitrate concentrations in the gas phase are significantly higher but other HOM monomers and dimers from monoterpene oxidation are lower at SORPES compared to SMEAR II. The model can simulate the NPF events at SMEAR II with a good agreement but underestimate the growth of new particles at SORPES, indicating a dominant role of sulfuric acid and HOM originated from oxidation of aromatics in the polluted environment. This study highlight the needs of molecular-scale measurements in improving the understanding of NPF mechanisms in the polluted areas like eastern China.

Atmospheric
Chemistry
and Physics
Discussions

1 Introduction

New particle formation (NPF), including the production of the molecular clusters and the subsequent growth of these clusters (Kulmala et al., 2014), is a global phenomenon and has been observed under different environmental conditions (Kulmala and Kerminen, 2008; Kulmala et al., 2004; Zhang et al., 2012).

5   NPF can influence climate by contributing to up to 50% of cloud condensation nuclei (CCN) (Merikanto et al., 2009; Sihto et al., 2011) and can have strong effects on air quality (Shen et al., 2011; Yu et al., 2010; Guo et al., 2014).

Sulfuric acid has been commonly considered as one of the main gas precursors of NPF (Kulmala and Kerminen, 2008;Zhang et al., 2012). Recently, it was found that HOM can participate in the initial steps of

10   NPF by stabilizing the sulfuric acid (Schobesberger et al., 2013;Riccobono et al., 2014;Kulmala et al., 2013). Most of the HOM dimers and the most oxidized monomers can be extremely low volatility organic compounds (ELVOCs) (Kurtén et al., 2016) and most likely contribute to the initial growth of newly formed particles (Trostl et al., 2016). Ehn et al. (2014) showed that monoterpene oxidation is a strong source of HOM and that these HOM can explain the majority of the observed particle growth from 2 nm up to 50 nm

15   in boreal forest. Recent studies (Jokinen et al., 2015;Trostl et al., 2016) showed that HOM can enhance atmospheric new particle formation and growth in most continental regions and increase the CCN concentrations by applying a constant monoterpene HOM yield (achieved from measurement) in a global model. Based on the HOM formation theory described by Ehn et al. (2014), a detailed HOM formation mechanism was applied (Öström et al., 2017; Roldin et al., 2018).

20   Currently, the role of HOM in NPF has been mainly studied in specific environment conditions with intensive observations available, such as the SMEAR II station in Nordic boreal forest (Ehn et al., 2014; Yan et al., 2016). However, understanding the mechanisms of NPF is particularly important from the perspective of air quality. As one of the most economically invigorating and densely populated countries, measurements of NPF events have been started since last decade in China (Shen et al., 2011; Wu et al.,

25   2007; Wang et al., 2017; Kivekas et al., 2009). Interestingly, the NPF events were observed frequently in heavily polluted environments in China (Qi et al., 2015; Kulmala et al., 2017; Wang et al., 2017). However, no measurements of HOM in China are reported until now and the understanding of the roles of HOM in NPF are very limited. The SORPES station at Nanjing is one of the "flagship" station in the domain of Pan-Eurasia Experiment (PEEX) (Kulmala et al., 2015; Lappalainen et al., 2016), providing a completely

30   different environment in comparison to the remote boreal forest. In this study, the NPF events at SMEAR II and SORPES, including the formation rates, growth rates and environmental conditions, were compared firstly. Then, by using the new version of the MALTE-BOX model, the precursor vapor gases (i.e. sulfuric acid and HOM) and NPF at two sites were simulated to deeply investigate the differences of NPF. This

modeling study will increase our understanding about NPF at an urban site in China and examines whether the nucleation and HOM formation mechanisms, which are intensively investigated at SMEAR II in Finland, can be used in polluted environment in China. In addition, applying a process model like MALTE-BOX, to simulate HOM concentrations and their contribution to the growth of newly formed particles at the two

5   selected sites with different environmental conditions, can validate whether a single HOM formation and nucleation mechanism could be appropriate in global models.

2 Materials and Methods

2.1 Sites and observations descriptions

SMEAR II station (Station for Measuring Forest Ecosystem-Atmosphere Relations) is located in

10   Hyytiälä, Finland (Fig. 1). The station is a boreal forest site, which is surrounded by a Scots pine forest with high monoterpene emissions. The SORPES station (Station for Observing Regional Processes of the Earth System) is located in Nanjing, eastern China (Fig. 1) (Ding et al., 2013; Ding et al., 2016). The station is a sub-urban site and about 20 km northeast of downtown Nanjing. The aerosol number size distributions, trace gases and meteorological parameters were continuously observed at both stations. Volatile organic

15   compounds (VOCs) were observed by PTR-MS at SMEAR II continuously at different altitudes. The HOM monomers (molecules with even mass in 300-450 Th), dimers (molecules with even mass in 452-620 Th), organonitrate (represented by seven major molecules, i.e. $C_7H_9O_8NNO_3^-$, $C_{10}H_{15}O_{6-11}NNO_3^-$) and sulfuric acid concentrations were measured at SMEAR II by CI-API-TOF (Jokinen et al., 2012) during spring 2013. At SORPES, VOCs were observed by GC-MS from September to October in 2014 (Xu et al., 2017). More

20   details about the two stations and measurements are described by Hari et al. (2013) and Ding et al. (2016).

2.2 Model descriptions

In this study we applied the MALTE-BOX model (the model to predict new aerosol formation in the lower troposphere), a zero-dimensional model, which includes several modules for the simulations of chemical and aerosol dynamical processes (Boy et al., 2006). This model has been successfully utilized in NPF

25   analysis - for instance, reproducing OH radical and gaseous sulfuric acid levels (Petäjä et al., 2009), validating various plausible nucleation mechanism and particle growth (Boy et al., 2007; Wang et al., 2013b), and identifying important factors influencing NPF occurrence (Boy et al., 2006; Boy et al., 2008; Ortega et al., 2012).

The gas-phase chemistry was simulated using the Master Chemical Mechanism version 3.3.1

30   (MCMv3.3.1, http://mcm.leeds.ac.uk/MCM/) solved by Kinetic PreProcessor (KPP) (Damian et al., 2002).

In addition, a new HOM autoxidation mechanism, which is constructed based on the oxidation of monoterpenes (Ehn et al., 2014), was added into the MCMv3.3.1. This HOM mechanism explicitly describes the HOM formation processes, i.e. ozone oxidation of monoterpenes, intramolecular H-shift and O_2 additions (autoxidation) (Öström et al., 2017; Roldin et al., 2018). Moreover, based on Molteni et al.

5   (2016), a simplified mechanisms of HOM formation from the oxidation of aromatics by OH were added into MCM3.3.1. The aerosol dynamical processes were simulated with the size-segregated aerosol model, UHMA (University of Helsinki Multicomponent Aerosol model) (Korhonen et al., 2004). A fixed sectional approach with 120 bins from 1 nm to 2.5 μm in diameter was used. For the smallest size bin, the formation rates of newly formed particles were estimated by the function of sulfuric acid and a first-generation

10   oxidation product of the included monoterpenes, i.e.

$$J_1 = k*[H_2SO_4][HOM_{nuc}],$$

where HOM_{nuc} was formed with a molar yield of 10^{-5} for each monoterpene reacted with OH (Roldin et al., 2015). The kinetic coefficient (k-value) was set for each case to achieve the highest correlation compared to the measured newly formed particles. Organic compounds with pure liquid saturation vapor pressure less

15   than 0.01 Pa were chosen as condensing vapors in UHMA. The saturation vapor pressures of organic compounds in MCMv3.3.1 were estimated with the group contribution method by Nannoolal et al. (2008) using the UManSysProp online system (Topping et al., 2016). The saturation vapor pressures of HOMs were calculated by SIMPOL (Pankow and Asher, 2008) as Nanoolal et al. (2008) method produces unrealistic estimates of vapor pressures for multifunctional HOMs containing hydroperoxide or peroxy acid

20   group (Kurtén et al., 2016). H_2SO_4 was treated as a non-volatile condensing vapor, which generally is a reasonable assumption at typical atmospheric relative humidity and NH_3 levels (Tsagkogeorgas et al., 2017). The coagulation process, dry deposition process and the dilution of aerosol number concentration caused by boundary layer evolution were estimated in the model as well.

The measurement variables, i.e. meteorological conditions (e.g. air temperature, relative humidity,

25   pressure and radiation), trace gases concentrations (e.g. SO_2, O_3, NO, NO_2, CO) and VOCs (e.g. ethylene, ethane, propane, acetone, methyl vinyl ketone, n-Butane, benzene, toluene, o-/m-xylene, 1,2,3/1,2,4-trimethylbenzene, ethylbenzene, isoprene and monoterpenes), were input into the MALTE-BOX model every 10 min. As monoterpenes were not measured by GC-MS at SORPES, monoterpene concentrations at SORPES were simulated using WRF-Chem, following the method of Huang et al. (2016), in which it was

30   shown that the MALTE-BOX model worked well in NPF simulation with WRF-Chem output of VOCs. The measured aerosol number size distribution was read into the model during the first five hours. The

Atmospheric
Chemistry
and Physics
Discussions

chemistry scheme was run with a spin up time of 24 hours, in order to achieve a realistic gas-phase composition before the aerosol module was switched on.

3 Results

3.1 Comparisons of NPF at SMEAR II and SORPES

5   According to long-term observations, the frequency of NPF at SMEAR II is 23%, with highest value in spring months (about 40-50%) (Nieminen et al., 2014). Although the concentration of pre-exiting particles is high, which inhibit NPF, the NPF occurs even more frequent in Chinese megacities such as Nanjing. The frequency of NPF at SORPES is 44%, with highest value also in spring month (55%) (Qi et al., 2015). As shown in Table 1, the averaged formation rate of 6 nm particles (J_6) at SMEAR II are 0.3 $cm^{-3}s^{-1}$ while the

10   J_6 at SORPES is 2.3 $cm^{-3}s^{-1}$ in average, which is almost 8 times higher than at SMEAR II. The growth rate of 6-30 nm particles (GR) is also higher at SORPES, with 4.5 nm/h at SMEAR II compared to 8.7 nm/h at SORPES in average.

    The environmental conditions during NPF at the two sites are substantially different. First, the pre-existing particle loading is much higher at SORPES than at SMEAR II. The CS at SORPES is almost 20

15   times higher than at SMEAR II (Table 1). High CS tends to inhibit the occurrence of NPF because of the scavenging of cluster and the loss of gas-phase low-volatility compounds (Kulmala et al., 2017). Secondly, the concentrations of atmospheric oxidant such as ozone are higher at SORPES (Table 1). Moreover, the concentrations of OH and NO_3 radical in YRD urban area of China are higher than the clean area (Wang et al., 2013a;Nan et al., 2017).Third, the anthropogenic pollutants are much higher at SORPES than at

20   SMEAR II. As an important gas precursor of NPF, the SO_2 concentration at SORPES is almost 50 times higher than at SMEAR II (Table 1). The concentration of NO_x, which is believed to suppress the NPF by reacting with peroxy radicals (Wildt et al., 2014), is also much higher at SORPES.

    To in depth study the differences of NPF at SMEAR II and SORPES, the four NPF days and one non-

25   NPF day at each site were chosen for simulations with MALTE-BOX (Table 2). Besides the differences of NPF parameters and environmental conditions at the two sites described above, monoterpene and benzene concentrations on each day at the two sites are tabulated in Table 2. Because of the high monoterpene emissions in southern China (Fig 1), the monoterpene concentrations are relatively high at SORPES especially when the air masses origin from south. The averaged monoterpene concentration on chosen days

30   is 0.05 ppbv at SORPES compared to 0.13 ppbv at SMEAR II. As a sub-urban site, the anthropogenic VOCs (e.g. benzene, Table 2) are higher at SORPES than at SMEAR II, with 0.54 ppbv of benzene concentration at SORPES compared to 0.06 ppbv at SMEAR II in average. The averaged concentration of aromatics

(including benzene, toluene, o-/m-xylene, 1,2,3/1,2,4-trimethylbenzene, ethylbenzene) at SORPES on chosen days was 1.2 ppbv.

3.2 The differences of simulated condensing vapors at two sites

As shown in Fig 2a, similar to previous studies (Zhou et al., 2014), the model underestimates the concentrations of sulfuric acid at SMEAR II especially at night. The reasons for this discrepancy could be that there are other oxidants besides OH and Criegee Intermediate radicals lead to the formation of sulfuric acid (Boy et al., 2013). Because of the detection limit of the CI-API-TOF, the HOMs non-nitrate monomers, dimers and organonitrates presented in Figs. 2b-d contain 7-14, 8-17, 7-14 oxygen atoms, respectively. The model predicts the measured diurnal cycle of HOM non-nitrate monomers at SMEAR II with good agreement. For HOM dimers, the simulated concentrations are higher than the measurements at night while slightly lower at daytime when the NPF events occur. For HOM organonitrate, although matching well with measurements at daytime, the simulation results have stronger diurnal pattern, with much lower concentrations than measurements at night. In general, the normalized mean bias (NMB) values of sulfuric acid, HOM non-nitrate monomers, dimers, organonitrates and total HOM are -63.0%, 11.1%, 174.3%, 8.0% and 38.3%, respectively. Considering the uncertainties of the CI-API-TOF in measuring gas HOM (estimated uncertainty up to a factor of 2-3) and the many unknowns in their formations, the model provides an acceptable agreement between simulated and measured vapor concentrations.

Although no measurements of sulfuric acid and HOM are conducted at SORPES, a comparison of the simulated gas vapors concentrations at two sites can help us to qualitatively understand the differences between the boreal forest and polluted areas in China. As shown in Fig. 2a, the simulated sulfuric acid at SORPES is one order of magnitude higher than at SMEAR II at daytime. The high value of sulfuric acid is mainly related to the extremely high SO_2 concentrations and high atmospheric oxidation capacity at SORPES. Such high simulated sulfuric acid concentration is consistent with the measurements conducted in other urban sites in China, e.g. about 10^7 #/cm^3 in Beijing (Wang et al., 2013b). The simulated HOM non-nitrate monomer concentrations from monoterpene oxidation are lower at SORPES (Fig. 2b) because of low values of monoterpene concentrations and high condensation sink. The simulated HOM dimer concentrations are much lower at SORPES than at SMEAR II while HOM organonitrate concentrations at SORPES are one order of magnitude higher than at SMEAR II (Fig. 2c, d). It is mainly because high NO concentrations at SORPES suppress the HOM dimer formation but contribute to the formation of HOM organonitrates.

As the comprehensive HOM formation mechanisms used in MALTE-BOX model are only based on the oxidation of monoterpenes, the simulated HOM monomer, dimer and organonitrate concentrations

presented above only refer to the HOM formed from monoterpene autoxidation. However, recent lab experiment shows that the aromatic hydrocarbons (e.g. benzene, toluene, o-/m-/p-xylene, 1,3,5-/1,2,3-/1,2,4-trimethylbenzene) oxidized by OH can lead to a subsequent autoxidation chain reaction forming HOM, which is believed to contribute substantially to NPF in urban area (Molteni et al., 2016). Therefore, according to Molteni et al. (2016), a HOM molar yield of 3% for the OH oxidation of the aromatic species was assumed and added into the MCMv3.3.1. The contributions of aromatics oxidation to the HOM can be ignored in the remote boreal forest because of extremely low aromatics concentrations. However, as shown in Fig 3, the HOM from aromatics oxidation at SORPES can be above 10^8 #/cm^3, which is about one magnitude higher than HOM from monoterpene oxidation. HOM concentration from aromatics oxidation on NPF days is obviously higher than non-event days, reflecting an important role of HOM in NPF. Such high concentration of HOM from aromatics oxidation is caused by the high levels of aromatics and OH radical in the polluted urban environment and may contribute substantially to the SOA formation.

3.3 The simulations of aerosol size distributions at two sites

Figure 4 shows the variations of measured and simulated aerosol number size distribution at SMEAR II and SORPES. The kinetic coefficients (k-value) on each day at both sites (tuned to cover the observed particle formation rates) is texted in Fig 4b and 4d. For the SMEAR II site, the model can capture both the NPF events and non-NPF events with same k-value, i.e. 1×10^{-18} m^3 s^{-1}. Comparing the observed and simulated formation rates of 6 nm particles at SMEAR II (Table 3), the model underestimated the formation rate on 1 May, 2013 but overestimated the formation on other NPF days. During event days, more than one banana shape was simulated at SMEAR II, which is mainly because of the multi-peaks of simulated sulfuric acid. For SORPES station, the k-value is higher than at SMEAR II in average and with more discrepancies. The k-value on 22 September, 2014 is more similar with the value at SMEAR II but much lower than other chosen days. The variations of the k-values can reflect the variability of other unaccounted compounds involved in the particle or cluster formation and initial growth (Kuang et al., 2008). As only HOM from monoterpene oxidation was involved in the nucleation mechanism of MALTE-BOX, the much higher k-values at SORPES except on 22 September, 2014 reflects that other compounds, which are most probable the oxidation products of anthropogenic pollutants, can also involve in the nucleation. Moreover, the model cannot simulate the high formation rates observed at SORPES except on 22 September, 2014 (Table 3).

For simulations at SORPES station, the brief formation mechanisms of HOM from aromatics were added in the MCM and the saturation vapor pressure of HOM were calculated by SIMPOL. However, even if we decrease the pure liquid saturation vapor pressures of HOM from aromatics oxidation with 2 orders of magnitude, the model underestimates the growth during the event days, except on 22 September, 2014.

The simulated growth rates on 22 and 24 September, 4 and 6 October are 7.8, 3.3, 2.8 and 2.8 nm/h, compared to the observed growth rates with 9.9, 16.2, 14.9 and 12.9 nm/h, respectively (Table 3). These results indicate that under polluted environmental condition there must be some other important gas vapors that are not accounted for in the model that contributes to the growth. Tao et al. (2016) found that

5   heterogeneous uptake of amines can effectively contribute to particle growth of newly formed particles in polluted YRD area of China. Comparing the averaged observed and simulated number size distribution (Fig 5), the simulated aerosol size distributions were in good agreement with measurements at SMEAR II, but the simulated number concentrations in the size range below 200 nm at SORPES are extremely lower than the observation. One reason is that primary particle emission is an important source of ultrafine particles in

10   urban areas (Qi et al., 2015), but not accounted in the model. Another reason is that current chemistry mechanisms and the accounted VOCs in the model dramatically underestimate secondary organic aerosol (SOA) formation in polluted area.

Only the NPF event on 22 September, 2014 was simulated in good agreement with measurement because this day had the lowest condensation sink and highest aromatics concentrations among the chosen

15   NPF cases at SORPES. Fig. 6 presents the footprints of all the cases at SORPES. The air mass on 22 September, 2014 was from marine area. Previous study shows that these marine air masses have the lowest accumulation mode particles concentrations and therefore the NPF occurs frequently (Qi et al., 2015). Although having the lowest condensation sink, the aromatics concentration on this day was still quite high, which was most probably emitted from local petrochemical industrial area. The air masses on 24 September

20   and 6 October were from North China and brought air pollutants to Nanjing (Figs. 6b, 6e). On 4 October, it had similar retroplumes with those on 22 September but with more local origin (Fig. 6). Holiday effects in China (National Holiday with more family vacations during 1-7 October) caused the high NO_x and anthropogenic VOCs concentrations on this day (Xu et al., 2017). The formation and growth of NPF were suppressed by high NO_x concentration and therefore cannot be simulated by current MALTE-BOX model.

25   **3.4 The differences of relative contributions of precursor vapors to growth at two sites**

Figure 7 shows the averaged relative contributions of precursor vapors to the growth of sub-100 nm particles from 9:00 to 15:00 LT during the four chosen NPF days at SMEAR II and on 22 September, 2014 at SORPES. Only the NPF event on 22 September, 2014 was presented at SORPES because current MALTE-BOX model can only capture the shape of NPF on this day. At SMEAR II, the growth of ultrafine particles

30   was dominated by HOM from monoterpene oxidation, which is consistent with the previous study by Ehn et al. (2014). HOM monomers contribute most to the growth at SMEAR II as they have high concentrations and relatively low saturation vapor pressures.

Atmospheric
Chemistry
and Physics
Discussions

The relative contributions of precursor vapors to the growth of particles at SORPES are quite different with those at SMEAR II. First, through the higher gas-phase sulfuric acid concentration at SORPES (as shown in Fig 2), sulfuric acid has huge contributions to the growth of ultrafine particles at SORPES while playing a minor role in the growth at SMEAR II. Second, high NO concentration at SORPES switches the

5   formation of HOM non-nitrate monomers and dimers to the formation of HOM organonitrates. As under the same oxygen to carbon ratio the saturation vapor pressures of organonitrates were higher than non-nitrate monomers and dimers, the HOMs from monoterpene oxidation contribute less to the growth at SORPES in general. Third, at SORPES, HOM from aromatics oxidation play a dominant role in the growth of ultrafine particles because of high aromatics concentrations. Dai et al. (2017) conducted the simultaneous

10   measurements near a petrochemical industrial area in Nanjing and found that the anthropogenic VOCs have significant contributions to both the nucleation and the growth. This is also consistent with the previous study at SORPES that higher growth rates were observed when the air masses were from the YRD area with high anthropogenic VOCs emissions (Qi et al., 2015).

4 Conclusions

15   Higher frequency, formation rates and growth rates of new particle formation (NPF) events were observed at SORPES, a sub-urban site in eastern China, compared to SMEAR II, a boreal forest site in Finland. To quantitatively understand the differences of NPF at the two sites, the condensing vapors (i.e. sulfuric acid and HOM) and particle number size distributions were simulated by a new version of MALTE-BOX model with the comprehensive HOM formation mechanism based on monoterpene oxidation and simplified

20   mechanism of HOM formation from aromatics oxidation.

The model was proved to work well on simulating the sulfuric acid and HOM from monoterpene oxidation by comparing them with measurements at SMEAR II. Comparing the simulated sulfuric acid and HOM from monoterpene oxidation at two sites, the sulfuric acid and HOM organonitrate concentrations were much higher while the concentrations of HOM non-nitrate monomers and dimers are lower at

25   SORPES than at SMEAR II. High concentration of HOM from aromatics oxidation were simulated at SORPES. The differences of gas vapors (sulfuric and HOM) at two sites are mainly because the substantially higher SO_2, NO, aromatics concentration and condensation sink at SORPES. The model can simulate the particle number size distributions on NPF and non-NPF days with same kinetic coefficient at SMEAR II. However, the k-value is more divergent at SORPES, which means the mechanism of nucleation

30   at polluted urban is more complicated. HOM from monoterpene oxidation contribute more to the growth at SMEAR II while the sulfuric acid and HOM from aromatics play dominant roles in the growth of newly formed particles at SORPES. This study highlights that sulfuric acid and HOM concentration and their

relative contributions to the growth are distinct at different environmental conditions. To better understand the formation mechanisms of secondary aerosols, sulfuric acid and HOM measurements in urban regions in China are needed.

References

Boy, M., Hellmuth, O., Korhonen, H., Nilsson, E. D., ReVelle, D., Turnipseed, A., Arnold, F., and Kulmala, M.: MALTE - model to predict new aerosol formation in the lower troposphere, Atmos. Chem. Phys., 6, 4499-4517,

20   2006.

Boy, M., Bonn, B., Kazil, J., Lovejoy, N., Turnipseed, A., Greenberg, J., Karl, T., Mauldin, L., Kusciuch, E., Smith, J., Barsanti, K., Guenther, A., Wehner, B., Hellmuth, O., Siebert, H., Bauer, S., Wiedensohler, A., and Kulmala, M.: Relevance of Several Nucleation Theories in Different Environments, in: Nucleation and Atmospheric Aerosols: 17th International Conference, Galway, Ireland, 2007, edited by: O'Dowd, C. D., and Wagner, P. E.,

25   Springer Netherlands, Dordrecht, 87-91, 2007.

Boy, M., Kazil, J., Lovejoy, E. R., Guenther, A., and Kulmala, M.: Relevance of ion-induced nucleation of sulfuric acid and water in the lower troposphere over the boreal forest at northern latitudes, Atmos. Res., 90, 151-158, 10.1016/j.atmosres.2008.01.002, 2008.

Boy, M., Mogensen, D., Smolander, S., Zhou, L., Nieminen, T., Paasonen, P., Plass-Dülmer, C., Sipilä, M., Petäjä, T.,

30   Mauldin, L., Berresheim, H., and Kulmala, M.: Oxidation of SO2 by stabilized Criegee intermediate (sCI) radicals as a crucial source for atmospheric sulfuric acid concentrations, Atmos. Chem. Phys., 13, 3865-3879, 10.5194/acp-13-3865-2013, 2013.

Dai, L., Wang, H., Zhou, L., An, J., Tang, L., Lu, C., Yan, W., Liu, R., Kong, S., and Chen, M.: Regional and local new particle formation events observed in the Yangtze River Delta region, China, J. Geophys. Res.- Atmos., 122, 2389-2402, 2017.

Dal Maso, M., Kulmala, M., Riipinen, I., Wagner, R., Hussein, T., Aalto, P. P., and Lehtinen, K. E. J.: Formation and

5   growth of fresh atmospheric aerosols: eight years of aerosol size distribution data from SMEAR II, Hyytiala, Finland, Boreal Environ. Res., 10, 323-336, 2005.

Damian, V., Sandu, A., Damian, M., Potra, F., and Carmichael, G. R.: The kinetic preprocessor KPP - a software environment for solving chemical kinetics, Comput. Chem. Eng., 26, 1567-1579, 10.1016/s0098-1354(02)00128-x, 2002.

10 Ding, A. J., Fu, C. B., Yang, X. Q., Sun, J. N., Zheng, L. F., Xie, Y. N., Herrmann, E., Nie, W., Petaja, T., Kerminen, V. M., and Kulmala, M.: Ozone and fine particle in the western Yangtze River Delta: an overview of 1 yr data at the SORPES station, Atmos. Chem. Phys., 13, 5813-5830, 10.5194/acp-13-5813-2013, 2013.

Ding, A. J., Nie, W., Huang, X., Chi, X., Sun, J., Kerminen, V.-M., Xu, Z., Guo, W., Petäjä, T., Yang, X., Kulmala, M., and Fu, C.: Long-term observation of air pollution-weather/climate interactions at the SORPES station: a

15   review and outlook, Front. Environ. Sci. & Eng., 10, 15, 10.1007/s11783-016-0877-3, 2016.

Ehn, M., Thornton, J. A., Kleist, E., Sipila, M., Junninen, H., Pullinen, I., Springer, M., Rubach, F., Tillmann, R., Lee, B., Lopez-Hilfiker, F., Andres, S., Acir, I. H., Rissanen, M., Jokinen, T., Schobesberger, S., Kangasluoma, J., Kontkanen, J., Nieminen, T., Kurten, T., Nielsen, L. B., Jorgensen, S., Kjaergaard, H. G., Canagaratna, M., Dal Maso, M., Berndt, T., Petaja, T., Wahner, A., Kerminen, V. M., Kulmala, M., Worsnop, D. R., Wildt, J., and

20   Mentel, T. F.: A large source of low-volatility secondary organic aerosol, Nature, 506, 476-+, 10.1038/nature13032, 2014.

Guo, S., Hu, M., Zamora, M. L., Peng, J. F., Shang, D. J., Zheng, J., Du, Z. F., Wu, Z., Shao, M., Zeng, L. M., Molina, M. J., and Zhang, R. Y.: Elucidating severe urban haze formation in China, Proceedings of the National Academy of Sciences of the United States of America, 111, 17373-17378, 10.1073/pnas.1419604111, 2014.

25 Hari, P., Nikinmaa, E., Pohja, T., Siivola, E., Bäck, J., Vesala, T., and Kulmala, M.: Station for Measuring Ecosystem-Atmosphere Relations: SMEAR, in: Physical and Physiological Forest Ecology, edited by: Hari, P., Heliövaara, K., and Kulmala, L., Springer Netherlands, Dordrecht, 471-487, 2013.

Huang, X., Zhou, L. X., Ding, A. J., Qi, X. M., Nie, W., Wang, M. H., Chi, X. G., Petaja, T., Kerminen, V. M., Roldin, P., Rusanen, A., Kulmala, M., and Boy, M.: Comprehensive modelling study on observed new particle formation

30   at the SORPES station in Nanjing, China, Atmos. Chem. Phys., 16, 2477-2492, 10.5194/acp-16-2477-2016, 2016.

Jokinen, T., Berndt, T., Makkonen, R., Kerminen, V. M., Junninen, H., Paasonen, P., Stratmann, F., Herrmann, H., Guenther, A. B., Worsnop, D. R., Kulmala, M., Ehn, M., and Sipila, M.: Production of extremely low volatile organic compounds from biogenic emissions: Measured yields and atmospheric implications, Proceedings of the National Academy of Sciences of the United States of America, 112, 7123-7128, 10.1073/pnas.1423977112, 2015.

35 Kivekas, N., Sun, J., Zhan, M., Kerminen, V. M., Hyvarinen, A., Komppula, M., Viisanen, Y., Hong, N., Zhang, Y., Kulmala, M., Zhang, X. C., Deli, G., and Lihavainen, H.: Long term particle size distribution measurements at Mount Waliguan, a high-altitude site in inland China, Atmos. Chem. Phys., 9, 5461-5474, 2009.

Korhonen, H., Lehtinen, K. E. J., and Kulmala, M.: Multicomponent aerosol dynamics model UHMA: model development and validation, Atmos. Chem. Phys., 4, 757-771, 10.5194/acp-4-757-2004, 2004.

Kuang, C., McMurry, P. H., McCormick, A. V., and Eisele, F. L.: Dependence of nucleation rates on sulfuric acid vapor concentration in diverse atmospheric locations, J. Geophys. Res.-Atmos., 113, 9, 10.1029/2007jd009253, 2008.

Kulmala, M., Vehkamaki, H., Petaja, T., Dal Maso, M., Lauri, A., Kerminen, V. M., Birmili, W., and McMurry, P. H.: Formation and growth rates of ultrafine atmospheric particles: a review of observations, J. Aerosol Sci., 35, 143-176, 10.1016/j.jaerosci.2003.10.003, 2004.

Kulmala, M., and Kerminen, V. M.: On the formation and growth of atmospheric nanoparticles, Atmos. Res., 90, 132-150, 10.1016/j.atmosres.2008.01.005, 2008.

Kulmala, M., Kontkanen, J., Junninen, H., Lehtipalo, K., Manninen, H. E., Nieminen, T., Petaja, T., Sipila, M., Schobesberger, S., Rantala, P., Franchin, A., Jokinen, T., Jarvinen, E., Aijala, M., Kangasluoma, J., Hakala, J., Aalto, P. P., Paasonen, P., Mikkila, J., Vanhanen, J., Aalto, J., Hakola, H., Makkonen, U., Ruuskanen, T., Mauldin, R. L., Duplissy, J., Vehkamaki, H., Back, J., Kortelainen, A., Riipinen, I., Kurten, T., Johnston, M. V., Smith, J. N., Ehn, M., Mentel, T. F., Lehtinen, K. E. J., Laaksonen, A., Kerminen, V. M., and Worsnop, D. R.: Direct Observations of Atmospheric Aerosol Nucleation, Science, 339, 943-946, 10.1126/science.1227385, 2013.

Kulmala, M., Petaja, T., Ehn, M., Thornton, J., Sipila, M., Worsnop, D. R., and Kerminen, V. M.: Chemistry of Atmospheric Nucleation: On the Recent Advances on Precursor Characterization and Atmospheric Cluster Composition in Connection with Atmospheric New Particle Formation, Ann. Rev. Phys. Chem., 65, 65, 21-37, 10.1146/annurev-physchem-040412-110014, 2014.

Kulmala, M., Lappalainen, H. K., Petäjä T., Kurten, T., Kerminen, V.-M., Viisanen, Y., Hari, P., Sorvari, S., Bäck, J., Bondur, V., Kasimov, N., Kotlyakov, V., Matvienko, G., Baklanov, A., Guo, H. D., Ding, A., Hansson, H.-C., and Zilitinkevich, S.: Introduction: The Pan-Eurasian Experiment (PEEX) – multidisciplinary, multiscale and multicomponent research and capacity-building initiative, Atmos. Chem. Phys., 15, 13085-13096, https://doi.org/10.5194/acp-15-13085-2015, 2015.

Kulmala, M., Kerminen, V. M., Petaja, T., Ding, A. J., and Wang, L.: Atmospheric gas-to-particle conversion: why NPF events are observed in megacities?, Faraday Discussions, 200, 271-288, 10.1039/c6fd00257a, 2017.

Kurtén, T., Tiusanen, K., Roldin, P., Rissanen, M., Luy, J.-N., Boy, M., Ehn, M., and Donahue, N.: α-Pinene autoxidation products may not have extremely low saturation vapor pressures despite high O: C ratios, J. Phys. Chem. A, 120, 2569-2582, 2016.

Lappalainen, H. K., Kerminen, V.-M., Petäjä T., Kurten, T., Baklanov, A., Shvidenko, A., Bäck, J., Vihma, T., Alekseychik, P., Andreae, M. O., Arnold, S. R., Arshinov, M., Asmi, E., Belan, B., Bobylev, L., Chalov, S., Cheng, Y., Chubarova, N., de Leeuw, G., Ding, A., Dobrolyubov, S., Dubtsov, S., Dyukarev, E., Elansky, N., Eleftheriadis, K., Esau, I., Filatov, N., Flint, M., Fu, C., Glezer, O., Gliko, A., Heimann, M., Holtslag, A. A. M., Hõrrak, U., Janhunen, J., Juhola, S., Järvi, L., Järvinen, H., Kanukhina, A., Konstantinov, P., Kotlyakov, V., Kieloaho, A.-J., Komarov, A. S., Kujansuu, J., Kukkonen, I., Duplissy, E.-M., Laaksonen, A., Laurila, T., Lihavainen, H., Lisitzin, A., Mahura, A., Makshtas, A., Mareev, E., Mazon, S., Matishov, D., Melnikov, V., Mikhailov, E., Moisseev, D.,

Nigmatulin, R., Noe, S. M., Ojala, A., Pihlatie, M., Popovicheva, O., Pumpanen, J., Regerand, T., Repina, I., Shcherbinin, A., Shevchenko, V., Sipilä, M., Skorokhod, A., Spracklen, D. V., Su, H., Subetto, D. A., Sun, J., Terzhevik, A. Y., Timofeyev, Y., Troitskaya, Y., Tynkkynen, V.-P., Kharuk, V. I., Zaytseva, N., Zhang, J., Viisanen, Y., Vesala, T., Hari, P., Hansson, H. C., Matvienko, G. G., Kasimov, N. S., Guo, H., Bondur, V.,

5   Zilitinkevich, S., and Kulmala, M.: Pan-Eurasian Experiment (PEEX): towards a holistic understanding of the feedbacks and interactions in the land–atmosphere–ocean–society continuum in the northern Eurasian region, Atmos. Chem. Phys., 16, 14421-14461, https://doi.org/10.5194/acp-16-14421-2016, 2016.

Merikanto, J., Spracklen, D. V., Mann, G. W., Pickering, S. J., and Carslaw, K. S.: Impact of nucleation on global CCN, Atmos. Chem. Phys., 9, 8601-8616, 10.5194/acp-9-8601-2009, 2009.

10   Molteni, U., Bianchi, F., Klein, F., El Haddad, I., Frege, C., Rossi, M. J., Dommen, J., and Baltensperger, U.: Formation of highly oxygenated organic molecules from aromatic compounds, Atmos. Chem. Phys. , 18, 11909-1921, 2018.

Nan, J., Wang, S., Guo, Y., Xiang, Y., and Zhou, B.: Study on the daytime OH radical and implication for its relationship with fine particles over megacity of Shanghai, China, Atmos. Environ., 154, 167-178, 2017.

15   Nannoolal, Y., Rarey, J., and Ramjugernath, D.: Estimation of pure component properties: Part 3. Estimation of the vapor pressure of non-electrolyte organic compounds via group contributions and group interactions, Fluid Phase Equilibria, 269, 117-133, 2008.

Nieminen, T., Asmi, A., Dal Maso, M., Aalto, P. P., Keronen, P., Petäjä, T., Kulmala, M., and Kerminen, V.-M.: Trends in atmospheric new-particle formation: 16 years of observations in a boreal-forest environment, Boreal

20   Environ. Res., 19 (Suppl. B): 191-214, 2014.

Ortega, I. K., Suni, T., Boy, M., Gronholm, T., Manninen, H. E., Nieminen, T., Ehn, M., Junninen, H., Hakola, H., Hellen, H., Valmari, T., Arvela, H., Zegelin, S., Hughes, D., Kitchen, M., Cleugh, H., Worsnop, D. R., Kulmala, M., and Kerminen, V. M.: New insights into nocturnal nucleation, Atmos. Chem. Phys., 12, 4297-4312, 10.5194/acp-12-4297-2012, 2012.

25   Öström, E., Putian, Z., Schurgers, G., Mishurov, M., Kivekäs, N., Lihavainen, H., Ehn, M., Rissanen, M. P., Kurtén, T., Boy, M., Swietlicki, E., and Roldin, P.: Modeling the role of highly oxidized multifunctional organic molecules for the growth of new particles over the boreal forest region, Atmos. Chem. Phys., 17, 8887-8901, 10.5194/acp-17-8887-2017, 2017.

Pankow, J. F., and Asher, W. E.: SIMPOL.1: a simple group contribution method for predicting vapor pressures and

30   enthalpies of vaporization of multifunctional organic compounds, Atmos. Chem. Phys., 8, 2773-2796, 10.5194/acp-8-2773-2008, 2008.

Petäjä, T., Mauldin, I. R. L., Kosciuch, E., McGrath, J., Nieminen, T., Paasonen, P., Boy, M., Adamov, A., Kotiaho, T., and Kulmala, M.: Sulfuric acid and OH concentrations in a boreal forest site, Atmos. Chem. Phys., 9, 7435-7448, 10.5194/acp-9-7435-2009, 2009.

35   Qi, X. M., Ding, A. J., Nie, W., Petaja, T., Kerminen, V. M., Herrmann, E., Xie, Y. N., Zheng, L. F., Manninen, H., Aalto, P., Sun, J. N., Xu, Z. N., Chi, X. G., Huang, X., Boy, M., Virkkula, A., Yang, X. Q., Fu, C. B., and Kulmala,

Atmospheric
Chemistry
and Physics
Discussions

Open Access

M.: Aerosol size distribution and new particle formation in the western Yangtze River Delta of China: 2 years of measurements at the SORPES station, Atmos. Chem. Phys., 15, 12445-12464, 10.5194/acp-15-12445-2015, 2015.

Riccobono, F., Schobesberger, S., Scott, C. E., Dommen, J., Ortega, I. K., Rondo, L., Almeida, J., Amorim, A., Bianchi, F., Breitenlechner, M., David, A., Downard, A., Dunne, E. M., Duplissy, J., Ehrhart, S., Flagan, R. C., Franchin, A., Hansel, A., Junninen, H., Kajos, M., Keskinen, H., Kupc, A., Kurten, A., Kvashin, A. N., Laaksonen, A., Lehtipalo, K., Makhmutov, V., Mathot, S., Nieminen, T., Onnela, A., Petaja, T., Praplan, A. P., Santos, F. D., Schallhart, S., Seinfeld, J. H., Sipila, M., Spracklen, D. V., Stozhkov, Y., Stratmann, F., Tome, A., Tsagkogeorgas, G., Vaattovaara, P., Viisanen, Y., Vrtala, A., Wagner, P. E., Weingartner, E., Wex, H., Wimmer, D., Carslaw, K. S., Curtius, J., Donahue, N. M., Kirkby, J., Kulmala, M., Worsnop, D. R., and Baltensperger, U.: Oxidation Products of Biogenic Emissions Contribute to Nucleation of Atmospheric Particles, Science, 344, 717-721, 10.1126/science.1243527, 2014.

Roldin, P., Liao, L., Mogensen, D., Dal Maso, M., Rusanen, A., Kerminen, V. M., Mentel, T. F., Wildt, J., Kleist, E., Kiendler-Scharr, A., Tillmann, R., Ehn, M., Kulmala, M., and Boy, M.: Modelling the contribution of biogenic volatile organic compounds to new particle formation in the Julich plant atmosphere chamber, Atmos. Chem. Phys., 15, 10777-10798, 10.5194/acp-15-10777-2015, 2015.

Roldin, P. et al.: Constraining the sources, sinks and contribution of highly oxygenated molecules to the growth of new particles over the Boreal forest region, manuscript in prep. for Proceedings of the National Academy of Sciences, 2018.

Schobesberger, S., Junninen, H., Bianchi, F., Lonn, G., Ehn, M., Lehtipalo, K., Dommen, J., Ehrhart, S., Ortega, I. K., Franchin, A., Nieminen, T., Riccobono, F., Hutterli, M., Duplissy, J., Almeida, J., Amorim, A., Breitenlechner, M., Downard, A. J., Dunne, E. M., Flagan, R. C., Kajos, M., Keskinen, H., Kirkby, J., Kupc, A., Kurten, A., Kurten, T., Laaksonen, A., Mathot, S., Onnela, A., Praplan, A. P., Rondo, L., Santos, F. D., Schallhart, S., Schnitzhofer, R., Sipila, M., Tome, A., Tsagkogeorgas, G., Vehkamaki, H., Wimmer, D., Baltensperger, U., Carslaw, K. S., Curtius, J., Hansel, A., Petaja, T., Kulmala, M., Donahue, N. M., and Worsnop, D. R.: Molecular understanding of atmospheric particle formation from sulfuric acid and large oxidized organic molecules, Proceedings of the National Academy of Sciences of the United States of America, 110, 17223-17228, 10.1073/pnas.1306973110, 2013.

Shen, X. J., Sun, J. Y., Zhang, Y. M., Wehner, B., Nowak, A., Tuch, T., Zhang, X. C., Wang, T. T., Zhou, H. G., Zhang, X. L., Dong, F., Birmili, W., and Wiedensohler, A.: First long-term study of particle number size distributions and new particle formation events of regional aerosol in the North China Plain, Atmos. Chem. Phys., 11, 1565-1580, 10.5194/acp-11-1565-2011, 2011.

Sihto, S. L., Mikkila, J., Vanhanen, J., Ehn, M., Liao, L., Lehtipalo, K., Aalto, P. P., Duplissy, J., Petaja, T., Kerminen, V. M., Boy, M., and Kulmala, M.: Seasonal variation of CCN concentrations and aerosol activation properties in boreal forest, Atmos. Chem. Phys., 11, 13269-13285, 10.5194/acp-11-13269-2011, 2011.

Tao, Y., Ye, X., Jiang, S., Yang, X., Chen, J., Xie, Y., and Wang, R.: Effects of amines on particle growth observed in new particle formation events, J. Geophys. Res.: Atmos., 121, 324-335, 2016.

Atmospheric
Chemistry
and Physics
Discussions

Topping, D., Barley, M., Bane, M. K., Higham, N., Aumont, B., Dingle, N., and McFiggans, G.: UManSysProp v1.0: an online and open-source facility for molecular property prediction and atmospheric aerosol calculations, Geosci. Model Dev., 9, 899-914, 10.5194/gmd-9-899-2016, 2016.

Trostl, J., Chuang, W. K., Gordon, H., Heinritzi, M., Yan, C., Molteni, U., Ahlm, L., Frege, C., Bianchi, F., Wagner, R., Simon, M., Lehtipalo, K., Williamson, C., Craven, J. S., Duplissy, J., Adamov, A., Almeida, J., Bernhammer, A. K., Breitenlechner, M., Brilke, S., Dias, A., Ehrhart, S., Flagan, R. C., Franchin, A., Fuchs, C., Guida, R., Gysel, M., Hansel, A., Hoyle, C. R., Jokinen, T., Junninen, H., Kangasluoma, J., Keskinen, H., Kim, J., Krapf, M., Kurten, A., Laaksonen, A., Lawler, M., Leiminger, M., Mathot, S., Mohler, O., Nieminen, T., Onnela, A., Petaja, T., Piel, F. M., Miettinen, P., Rissanen, M. P., Rondo, L., Sarnela, N., Schobesberger, S., Sengupta, K., Sipila, M., Smith, J. N., Steiner, G., Tome, A., Virtanen, A., Wagner, A. C., Weingartner, E., Wimmer, D., Winkler, P. M., Ye, P. L., Carslaw, K. S., Curtius, J., Dommen, J., Kirkby, J., Kulmala, M., Riipinen, I., Worsnop, D. R., Donahue, N. M., and Baltensperger, U.: The role of low-volatility organic compounds in initial particle growth in the atmosphere, Nature, 533, 527-+, 10.1038/nature18271, 2016.

Tsagkogeorgas, G., Roldin, P., Duplissy, J., Rondo, L., Tröstl, J., Slowik, J. G., Ehrhart, S., Franchin, A., Kürten, A., and Amorim, A.: Evaporation of sulfate aerosols at low relative humidity, Atmos. Chem. Phys., 17, 8923-8938, 2017.

Wang, S., Shi, C., Zhou, B., Zhao, H., Wang, Z., Yang, S., and Chen, L.: Observation of NO3 radicals over Shanghai, China, Atmos. Environ., 70, 401-409, 2013a.

Wang, Z. B., Hu, M., Mogensen, D., Yue, D. L., Zheng, J., Zhang, R. Y., Liu, Y., Yuan, B., Li, X., Shao, M., Zhou, L., Wu, Z. J., Wiedensohler, A., and Boy, M.: The simulations of sulfuric acid concentration and new particle formation in an urban atmosphere in China, Atmos. Chem. Phys., 13, 11157-11167, 10.5194/acp-13-11157-2013, 2013b.

Wang, Z. B., Wu, Z., Yue, D., Shang, D., Guo, S., Sun, J., Ding, A., Wang, L., Jiang, J., Guo, H., Gao, J., Cheung, H. C., Morawska, L., Keywood, M., and Hu, M.: New particle formation in China: Current knowledge and further directions, Sci. Tot. Environ., 577, 258-266, 10.1016/j.scitotenv.2016.10.177, 2017.

Wildt, J., Mentel, T. F., Kiendler-Scharr, A., Hoffmann, T., Andres, S., Ehn, M., Kleist, E., Müsgen, P., Rohrer, F., Rudich, Y., Springer, M., Tillmann, R., and Wahner, A.: Suppression of new particle formation from monoterpene oxidation by NOx, Atmos. Chem. Phys., 14, 2789-2804, 10.5194/acp-14-2789-2014, 2014.

Wu, Z. J., Hu, M., Liu, S., Wehner, B., Bauer, S., Ssling, A. M., Wiedensohler, A., Petaja, T., Dal Maso, M., and Kulmala, M.: New particle formation in Beijing, China: Statistical analysis of a 1-year data set, J. Geophys. Res.-Atmos., 112, 10, 10.1029/2006jd007406, 2007.

Xu, Z., Huang, X., Nie, W., Chi, X., Xu, Z., Zheng, L., Sun, P., and Ding, A.: Influence of synoptic condition and holiday effects on VOCs and ozone production in the Yangtze River Delta region, China, Atmos. Environ., 168, 112-124, https://doi.org/10.1016/j.atmosenv.2017.08.035, 2017.

Yan, C., Nie, W., Äijälä, M., Rissanen, M. P., Canagaratna, M. R., Massoli, P., Junninen, H., Jokinen, T., Sarnela, N., Häme, S. A. K., Schobesberger, S., Canonaco, F., Yao, L., Prévôt, A. S. H., Petäjä, T., Kulmala, M., Sipilä, M., Worsnop, D. R., and Ehn, M.: Source characterization of highly oxidized multifunctional compounds in a boreal

forest environment using positive matrix factorization, Atmos. Chem. Phys., 16, 12715-12731, 10.5194/acp-16-12715-2016, 2016.

Yu, F. Q., Luo, G., Bates, T. S., Anderson, B., Clarke, A., Kapustin, V., Yantosca, R. M., Wang, Y. X., and Wu, S. L.: Spatial distributions of particle number concentrations in the global troposphere: Simulations, observations, and implications for nucleation mechanisms, J. Geophys. Res.-Atmos., 115, 14, 10.1029/2009jd013473, 2010.

Zhang, R. Y., Khalizov, A., Wang, L., Hu, M., and Xu, W.: Nucleation and Growth of Nanoparticles in the Atmosphere, Chem. Rev., 112, 1957-2011, 10.1021/cr2001756, 2012.

Zhou, L. X., Nieminen, T., Mogensen, D., Smolander, S., Rusanen, A., Kulmala, M., and Boy, M.: SOSAA - a new model to simulate the concentrations of organic vapours, sulphuric acid and aerosols inside the ABL - Part 2: Aerosol dynamics and one case study at a boreal forest site, Boreal Environ. Res., 19, 237-256, 2014.
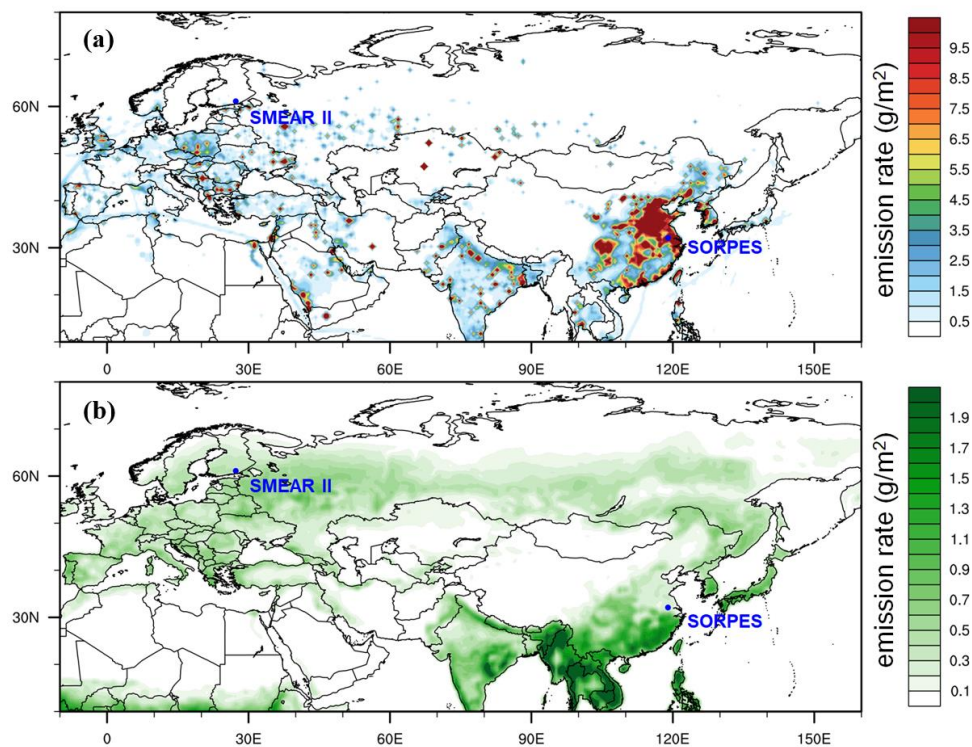
Atmospheric
Chemistry
and Physics
Discussions

Figure 1. Sites (SMEAR II and SORPES) locations on map of emission inventory of (a) SO_2 and (b) monoterpenes.

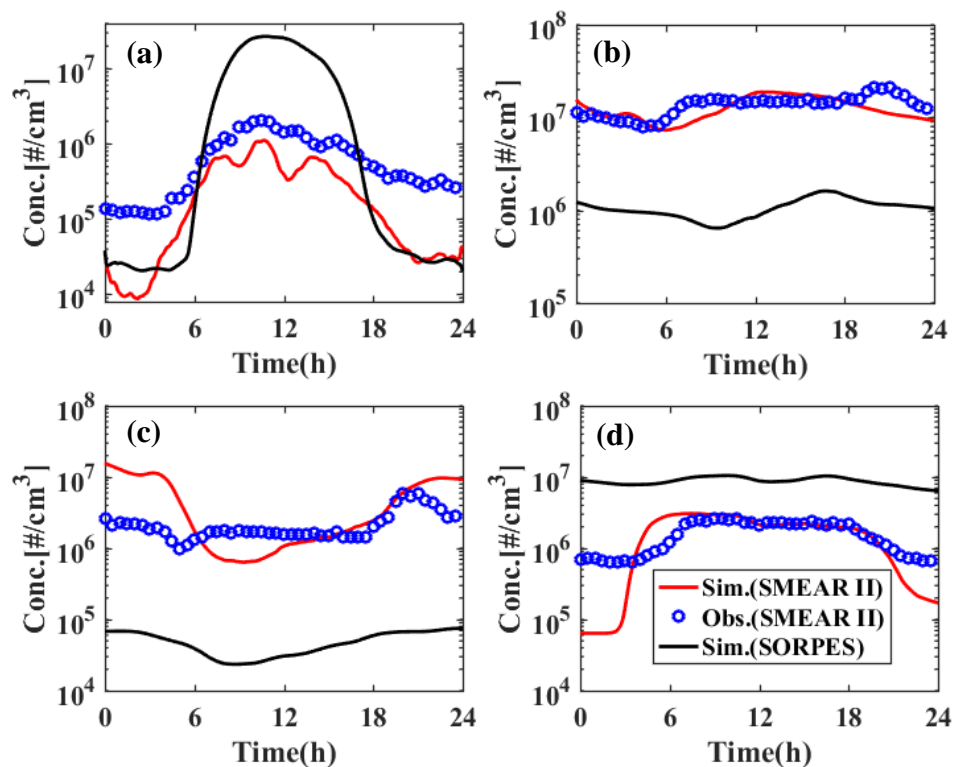Atmospheric
Chemistry
and Physics
Discussions

Figure 2. Averaged simulated and measured diurnal cycles of (a) H_2SO_4, (b) HOM non-nitrate monomers, (c) HOM dimers and (d) HOM organonitrates at SMEAR II and SORPES.
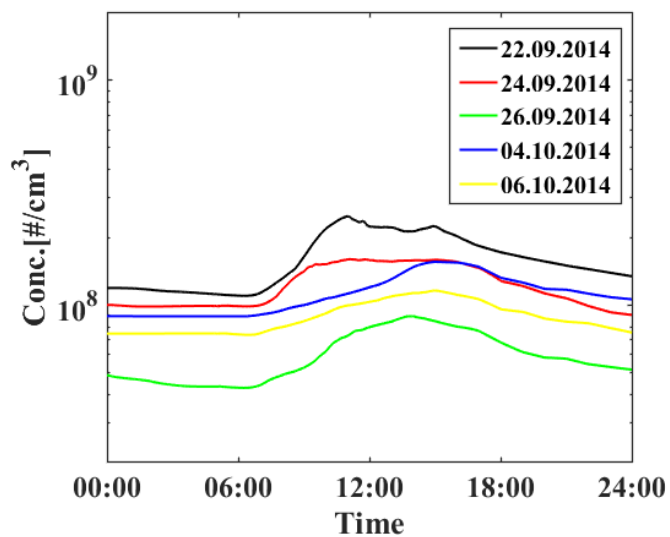
Figure 3. Simulated diurnal cycles of HOM formed from aromatics oxidation at SORPES on each chosen day.
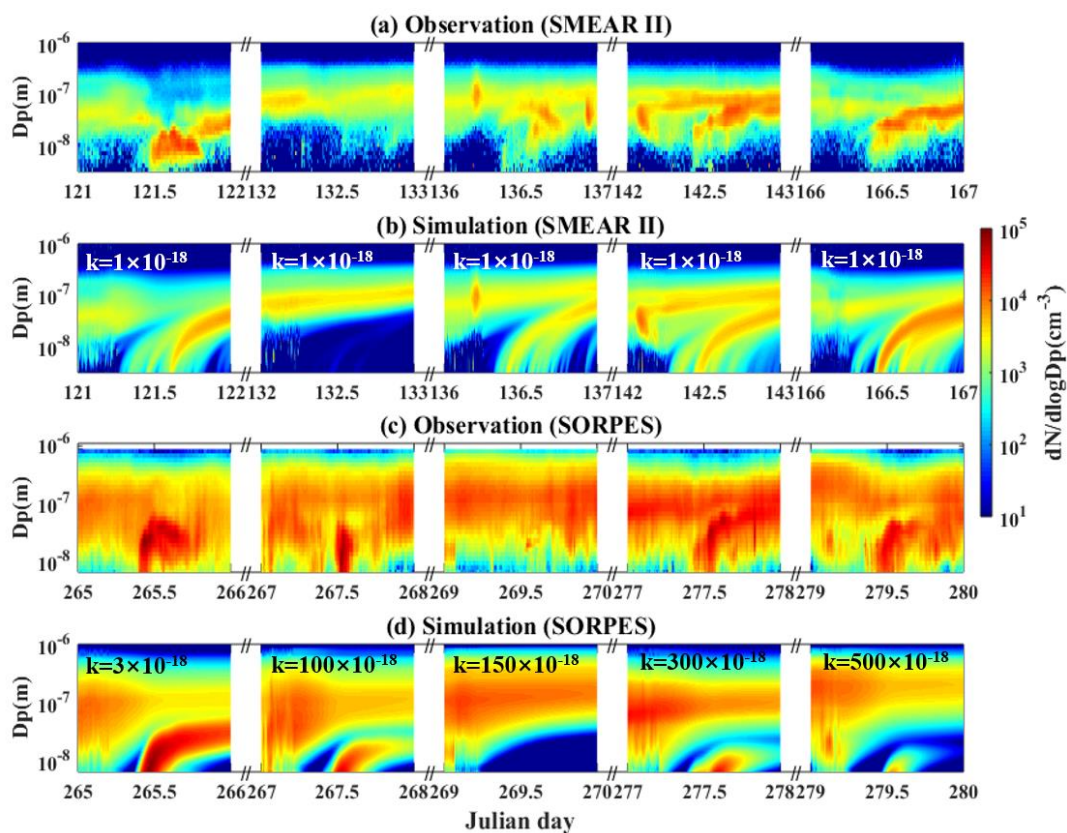
Figure 4. (a, c) Measured and (b, d) simulated particle number size distribution at SMEAR II and SORPES, respectively. Note: the kinetic coefficient on each day is texted in Figs. 2b & 2d.
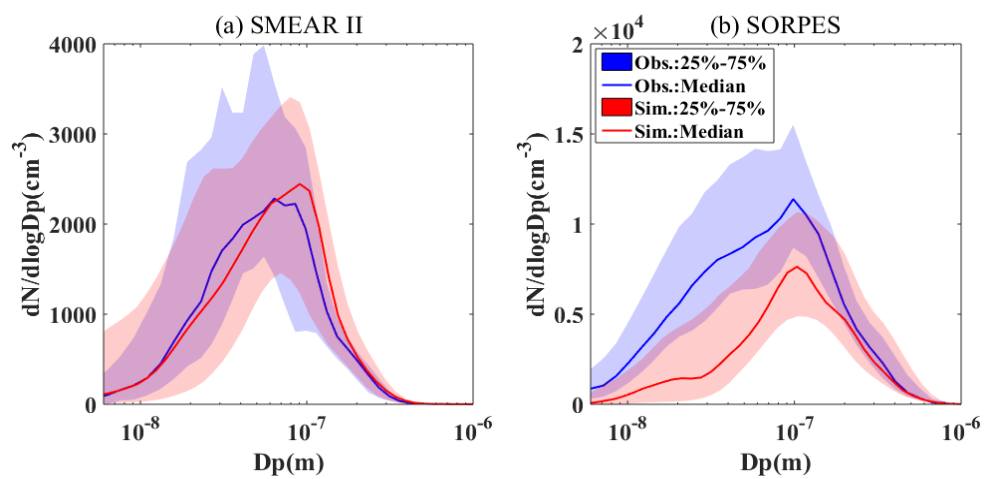
Figure 5. The observed and simulated aerosol number size distributions (a) at SMEAR II and (b) at SORPES. Note: Observed and simulated average (line) and ±1 standard deviation (shaded area) are in blue and red, respectively.
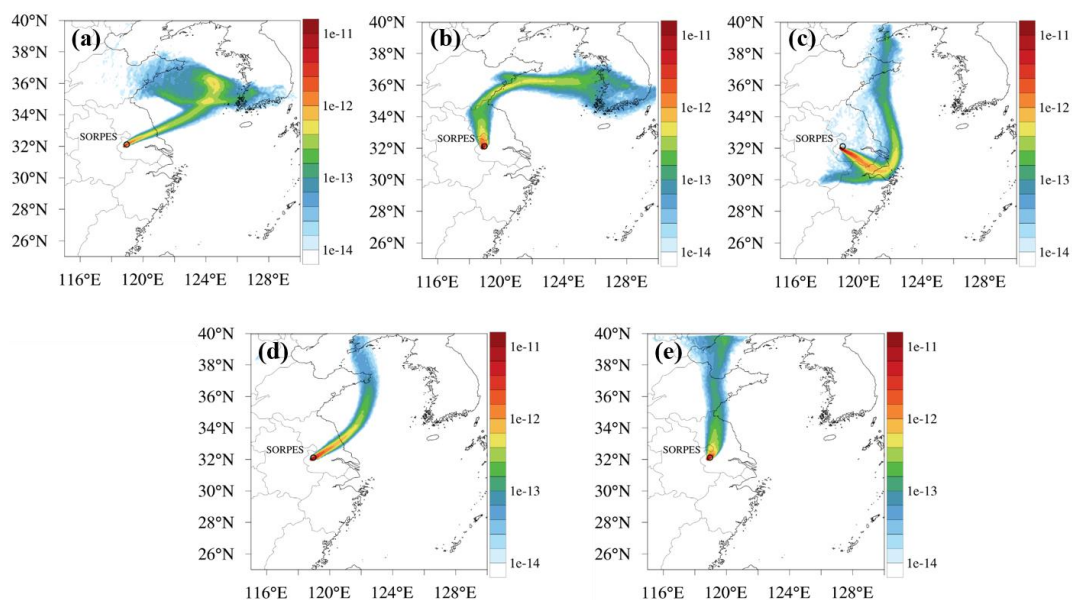
Figure 6. The averaged retroplume (footprint residence time) from 9:00 L.T. to 15:00 L.T. on (a) 22 September, (b) 24 September, (c) 26 September, (d) 4 October and (e) 6 October, 2014.
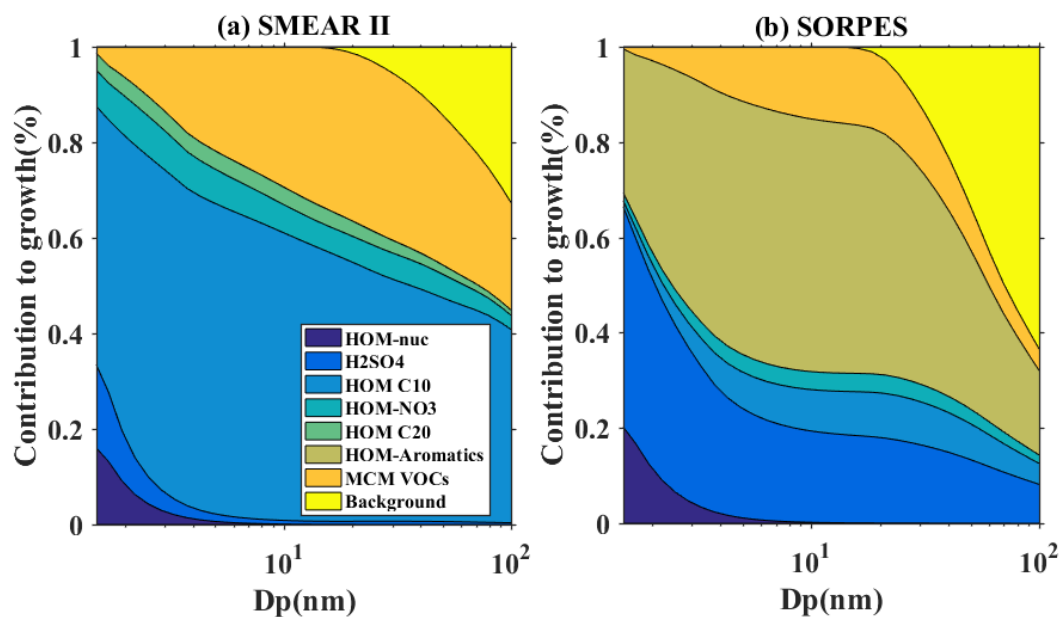
Figure 7. The relative contributions of precursor vapors to the growth of sub-100 nm particles at (a) SMEAR II and (b) SORPES.

Table 1. The statistics of observed formation rates of 6 nm particles (J_6), growth rates of 6-30 nm particles (GR) and condensation sinks (CS), O_3, SO_2, NO_x concentrations from 9:00 LT to 15:00 LT on NPF days at SMEAR II and SORPES. Note: The statistical samples are the whole year database of 2013 at SMEAR II and the whole year database of 2014 at SORPES.

	SMEAR II				SORPES			
	Average	Median	25th	75th	Average	Median	25th	75th
J_6 (cm^{-3}s^{-1})	0.3	0.1	0.06	0.3	2.3	1.6	1	3.5
GR (nm/h)	4.5	2.8	2.0	5.6	8.7	8.0	6.5	10.4
CS (10^{-2}s^{-1})	0.18	0.14	0.08	0.24	3.0	2.7	2.1	3.6
O_3 (ppbv)	36.1	36.6	29.6	41.8	44.7	43.3	28.0	59.1
SO_2 (ppbv)	0.2	0.1	0.03	0.3	9.4	8.0	4.4	12.7
NO_x (ppbv)	0.5	0.2	0.06	0.6	17.7	13.4	7.9	23.0

5

Atmospheric
Chemistry
and Physics
Discussions

Table 2. The NPF classification and environmental conditions on each chosen case day at SMEAR II and SORPES.
Note: Condensation sink, meteorological conditions and the concentrations of trace gases are from 9:00 L.T. to
15:00 L.T.

Case	NPF Classification	CS (10^{-2} s^{-1})	Temp (ºC)	Rad (W/m^2)	RH (%)	O$_3$ (ppbv)	SO$_2$ (ppbv)	NO$_x$ (ppbv)	Mono (ppbv)	Benz. (ppbv)
SMEAR II										
05/01/2013	NPF	0.06	7.1	605.1	41.1	36.0	0.03	0.05	0.05	0.08
05/12/2013	Non-NPF	0.3	13.8	553.2	43.0	40.4	0.07	0.08	0.1	0.06
05/16/2013	NPF	0.3	17.6	682.9	27.9	53.2	0.05	0.1	0.2	0.05
05/22/2013	NPF	0.3	16.3	471.7	40.7	35.7	0.2	0.1	0.2	0.06
06/15/2013	NPF	0.1	14.8	486.6	59.0	32.3	0.04	0.07	0.1	0.04
SORPES										
09/22/2014	NPF	2.1	24.6	497.0	60.2	45.2	2.4	7.7	0.04	0.7
09/24/2014	NPF	2.8	25.5	550.5	64.3	44.6	2.5	5.8	0.05	0.4
09/26/2014	Non-NPF	5.5	24.5	298.4	72.5	46.2	5.5	8.8	0.1	0.7
10/04/2014	NPF	2.5	22.2	567.6	53.7	36.2	8.3	22.2	0.04	0.6
10/06/2014	NPF	2.2	20.4	561.4	48.3	41.6	4.1	6.9	0.02	0.3

5

Atmospheric
Chemistry
and Physics
Discussions

Table 3. The observed and simulated formation rates of 6 nm particles (J6) and growth rates of 6-30 nm particles (GR) on chosen NPF days at each site.

	J_6 obs. $(cm^{-3}s^{-1})$	J_6 sim. $(cm^{-3}s^{-2})$	GR obs. (nm/h)	GR sim. (nm/h)
SMEAR II				
05/01/2013	0.6	0.3	3.8	3.7
05/16/2013	0.06	0.07	3.3	3.6
05/22/2013	0.05	0.3	4.0	4.5
06/15/2013	0.08	0.6	5.2	4.8
SORPES				
09/22/2014	4.9	5.6	9.9	7.8
09/24/2014	6.9	2.2	16.2	3.3
10/04/2014	3.8	1.8	14.9	2.8
10/06/2014	2.9	0.4	12.9	2.8